Ecological Complexity 23 (2015) 1–13

Contents lists available at ScienceDirect

Ecological Complexity

journal homepage: www.elsevier.com/locate/ecocom

Original Research Article

Improving the light use efficiency model for simulating terrestrial vegetation gross primary production by the inclusion of diffuse radiation across ecosystems in China

Shaoqiang Wang [a], Kun Huang [a,b,*], Hao Yan [c], Huimin Yan [a], Lei Zhou [a], Huimin Wang [a], Junhui Zhang [d], Junhua Yan [e], Liang Zhao [f], Yanfen Wang [b], Peili Shi [a], Fenghua Zhao [a], Leigang Sun [g]

[a] Key Laboratory of Ecosystem Network Observation and Modeling, Institute of Geographic Sciences and Natural Resources Research, Chinese Academy of Sciences, Beijing 100101, China
[b] University of Chinese Academy of Sciences, Beijing 100049, China
[c] National Meteorological Center, China Meteorological Administration, Beijing 100081, China
[d] Institute of Applied Ecology, Chinese Academy of Sciences, Shenyang 110016, China
[e] South China Botanical Garden, Chinese Academy of Sciences, Guangzhou 510650, China
[f] Northwest Plateau Institute of Biology, Chinese Academy of Sciences, Xining 810001, China
[g] Institute of Geographical Sciences, Hebei Academy of Sciences, Shijiazhuang 050000, China

ARTICLE INFO

Article history:
Received 5 November 2014
Received in revised form 10 April 2015
Accepted 27 April 2015
Available online 1 June 2015

Keywords:
Cloudiness index
Cloudiness index light use efficiency (CI-LUE) model
Eddy covariance flux
MOD17 model

ABSTRACT

Qualification of gross primary production (GPP) of terrestrial ecosystem over large areas is important in understanding the response of terrestrial ecosystem to global climate change. While light use efficiency (LUE) models were widely used in regional carbon budget estimates, few studies consider the effect of diffuse radiation on LUE caused by clouds using a big leaf model. Here we developed a cloudiness index light use efficiency (CI-LUE) model based on the MOD17 model algorithm to estimate the terrestrial ecosystem GPP, in which the base light use efficiency encompassed the cloudiness index, maximum LUE and clear sky LUE. GPP measured at seven sites from 2003 to 2007 in China were used to calibrate and validate the CI-LUE model. The results showed that at forest sites and cropland site the CI-LUE model outperformed the Vegetation Photosynthesis Model (VPM), Terrestrial Ecosystem Carbon flux model (TEC), MOD17 model algorithm driven by in situ meteorological measurements and MODIS GPP products, especially the R^2 of simulated GPP against flux measurements at Dinghushan forest site increased from 0.17 (MODIS GPP products) to 0.61 (CI-LUE). Instead, VPM model had the best agreement with GPP measurements followed by CI-LUE model and lastly TEC model at two grassland sites. Meanwhile, GPP calculated by CI-LUE model has less underestimation under cloudy skies in comparison with MOD17 model. This study demonstrated the potential of the CI-LUE model in improving GPP simulations resulting from the inclusion of diffuse radiation in regulating the base light use efficiency and maximum light use efficiency.

1. Introduction

Terrestrial ecosystems play an increasingly important role in global carbon cycle under climate change (Nemani et al., 2003). Gross primary production (GPP) is defined as the overall photosynthetically fixation of carbon per unit space and time (Monteith, 1972), which also represents the critical flux component that drives the terrestrial ecosystem carbon cycle. Subtle fluctuations in GPP have substantial implications for future climate warming scenarios (Cai et al., 2014; Raupach et al., 2008). With the quantification of GPP and net ecosystem exchange (NEE) of terrestrial ecosystem for regions, continents, or the globe, we can gain insight into the feedbacks between the terrestrial biosphere and the atmosphere under global change and climate policy-making facilitation (Wu et al., 2010a; Xiao et al., 2008).

* Corresponding author at: Key Laboratory of Ecosystem Network Observation and Modeling, Institute of Geographic Sciences and Natural Resources Research, Chinese Academy of Sciences, Beijing 100101, China. Tel.: +86 1064889809.
E-mail address: huangkuncas@163.com (K. Huang).

http://dx.doi.org/10.1016/j.ecocom.2015.04.004
1476-945X/

The eddy covariance (EC) technique provides the best way to measure NEE continuously that can be used for GPP calculation by subtracting the modeled ecosystem respiration components (Baldocchi et al., 2001; Wu et al., 2010a; Yu et al., 2006, 2013). Furthermore, the EC measurements only provide integrated CO_2 flux measurements over the tower footprint ranging from a hundred meters to several kilometers at the ecosystem level (Gockede et al., 2008; Osmond et al., 2004). Satellite remote sensing can provide consistent observation of vegetation over large areas, and has been reported to be widely used for characterization of canopy structure and GPP estimation that can overcome the lack of extensive EC flux tower measurements (Running et al., 2000; Wu et al., 2010a). Therefore, a number of modeling approaches have been developed for regional/global GPP estimations, including ecological process-based models and light use efficiency (LUE) models driven by remote sensing data (He et al., 2013). Among all the models, LUE models encompassing the LUE algorithm proposed by Monteith (1972) enjoy the popularity to identify the spatio-temporal dynamics of GPP due to the simplicity of concept and availability of remote sensing data (Ogutu and Dash, 2013). Various LUE models have been developed for this purpose, including MOD17 model (Heinsch et al., 2003; Running et al., 2004), Vegetation Photosynthesis Model (VPM) (Xiao et al., 2004), EC-LUE model (Yuan et al., 2007), Vegetation Index (VI) model (Wu et al., 2010b), C-Fix model (Veroustraete et al., 2002), Temperature and Greenness Rectangle (TGR) model (Yang et al., 2013). Recent studies indicated that GPP and LUE were affected by both the quantity and composition of the incoming solar radiation (Farquhar and Roderick, 2003; Gu et al., 2003; He et al., 2013; Kanniah et al., 2010, 2012, 2013; Mercado et al., 2009; Turner et al., 2006b). With a given value of total incoming radiation, LUE of entire canopy will increase with the increasing fraction of diffuse radiation that lead to an increment of the canopy fraction that is receiving illumination without photo-saturation (Mercado et al., 2009; Oliphant et al., 2011; Roderick et al., 2001; Sakowska et al., 2014). Under cloudy or aerosol-laden skies, incoming radiation was more diffuse and more uniformly distributed in the canopy with a smaller fraction of the canopy that was light saturated (He et al., 2013; Roderick et al., 2001). Consequently, canopy photosynthesis was inclined to be more light-use efficient under diffuse sunlight than under direct sunlight conditions (Gu et al., 2002, 2003; He et al., 2013; Kanniah et al., 2013; Mercado et al., 2009; Misson et al., 2005; Oliphant et al., 2011; Urban et al., 2014). Predictions showed that global secondary organic aerosols in the atmosphere will increase by 36% in 2100 (Heald et al., 2008). The aerosol influenced the cloud formation, which was the main contributor to the increment on diffuse radiation fraction (DRF) in the atmosphere (Feddema et al., 2005; Kim et al., 2005; Schiermeier, 2006). Furthermore, an increasing trend of annual diffuse radiation in China has been found to be 7.03 MJ m^{-2} yr^{-1} per decade from 1981 to 2010 (Ren et al., 2013). A two-leaf light use efficiency (TL-LUE) model was developed to address the effect of the sky condition and fraction of diffuse radiation on LUE modeling by stratifying the canopy into sunlit and shaded leaves (He et al., 2013). Based on the application of Farquhar's equations and assumption that a plant canopy functioned like a single big leaf (Farquhar et al., 1980), many big-leaf models (e.g. BIOME-BGC, TURC, DNDC, EDCM, ISAM, ORCHIDEE) were developed to simulate the canopy photosynthesis and ecosystem productivity (Chen et al., 1999; Kimball et al., 1997; Krinner et al., 2005; Li et al., 2010; Liu et al., 2003; Ruimy et al., 1996; Schaefer et al., 2012; Yang et al., 2009). However, few studies on ecosystem GPP predictions took into account effects of the DRF variations of the incoming radiation on LUE using a big leaf model based on the LUE concept. Previous studies have incorporated the diffuse radiation resulting from clouds and aerosols into the terrestrial plant productivity simulation by land surface process models (Kanniah et al., 2012), including isotope-enabled land surface model (ISOLSM) (Still et al., 2009), JULES land surface model (Alton et al., 2007; Mercado et al., 2009), CERES crop model (Greenwald et al., 2006), and CSU unified land model (Matsui et al., 2008). Moreover, with the great carbon sequestration potential of the terrestrial ecosystem of China in global carbon budget (Piao et al., 2009), large uncertainties still existed in terrestrial ecosystem LUE model for GPP simulations.

In order to quantify the effect of components variation of incoming radiation, the cloud condition which can result in overcast skies or clear skies should be taken into account in GPP modeling. A cloudiness index derived from digital elevation model was used to indicate the fraction of diffuse radiation in the radiation absorbed by the vegetation photosynthesis. Here we employed flux measurements from 7 sites of ChinaFLUX, a cloudiness index-light use efficiency (CI-LUE) model of GPP based on the CFLUX model and MOD17 model (Running et al., 2004; Turner et al., 2006b) to predict the GPP with a simple data assimilation approach. The objectives of this study are to: (1) calibrate and evaluate CI-LUE model against EC flux measurements and other LUE models; (2) quantify the sensitivity of CI-LUE modeling performance to variation of diffuse radiation fraction; (3) test the hypothesis that inclusion of diffusion radiation could improve the light use efficiency model for GPP estimations.

2. Materials and methods

2.1. Eddy flux observations

Carbon flux data (GPP and NEE) observed continuously at 7 typical sites across China were applied to model calibration and validation in this study (Fig. 1). The main information on location, vegetation and climate of those 7 sites are summarized in Table 1.

The open-path eddy covariance (OPEC) system was used to measure carbon and water vapor fluxes at ChinaFLUX sites. The OPEC system consists of and open-path infrared gas analyzer (Model LI-7500, LICOR Inc., Lincoln, NE, USA) and a 3-D sonic anemometer (Model CSAT3, Campbell Scientific Inc., Logan, UT, USA). The signals of the instruments were recorded at 10 Hz by a CR5000 datalogger (Model CR5000, Campell Scientific Inc.) and then block-averaged over 30-min intervals for analyses and archiving (Fu et al., 2006a; Guan et al., 2006; Yu et al., 2008b). The routine meteorological variables were measured simultaneously at 30-min intervals with dataloggers, including solar moisture, air temperature, rainfall, soil temperature, and soil moisture.

ChinaFLUX developed a series of proven methodologies for assessing the performance of observation system and flux data quality control including coordinate rotation, WPL correction, canopy storage calculation, nighttime flux correction, and gap filling and flux partitioning (Yu et al., 2006, 2013). Prior to conducting the scalar flux computation, three-dimensional rotation of the coordinate was applied to wind components to remove the effect of the instrument tilt or irregularity on airflow. The WPL correction was then applied to adjust the effect of air density caused by the transfer of heat and water vapor with the method described by Webb et al. (1980). Storage flux was calculated and the abnormal values were eliminated. The nighttime CO_2 flux data under low atmospheric turbulence conditions were screened using site-specific threshold of friction velocity (u_*), which was identified with the method described by Reichstein et al. (2005). The data gaps were filled with the nonlinear regression method suggested by Falge et al. (2001). Then we got continuous 30 min flux data.

The flux of net ecosystem CO_2 exchange (NEE, mg CO_2 m^{-2} s^{-1}) between the ecosystem and the atmosphere was calculated with

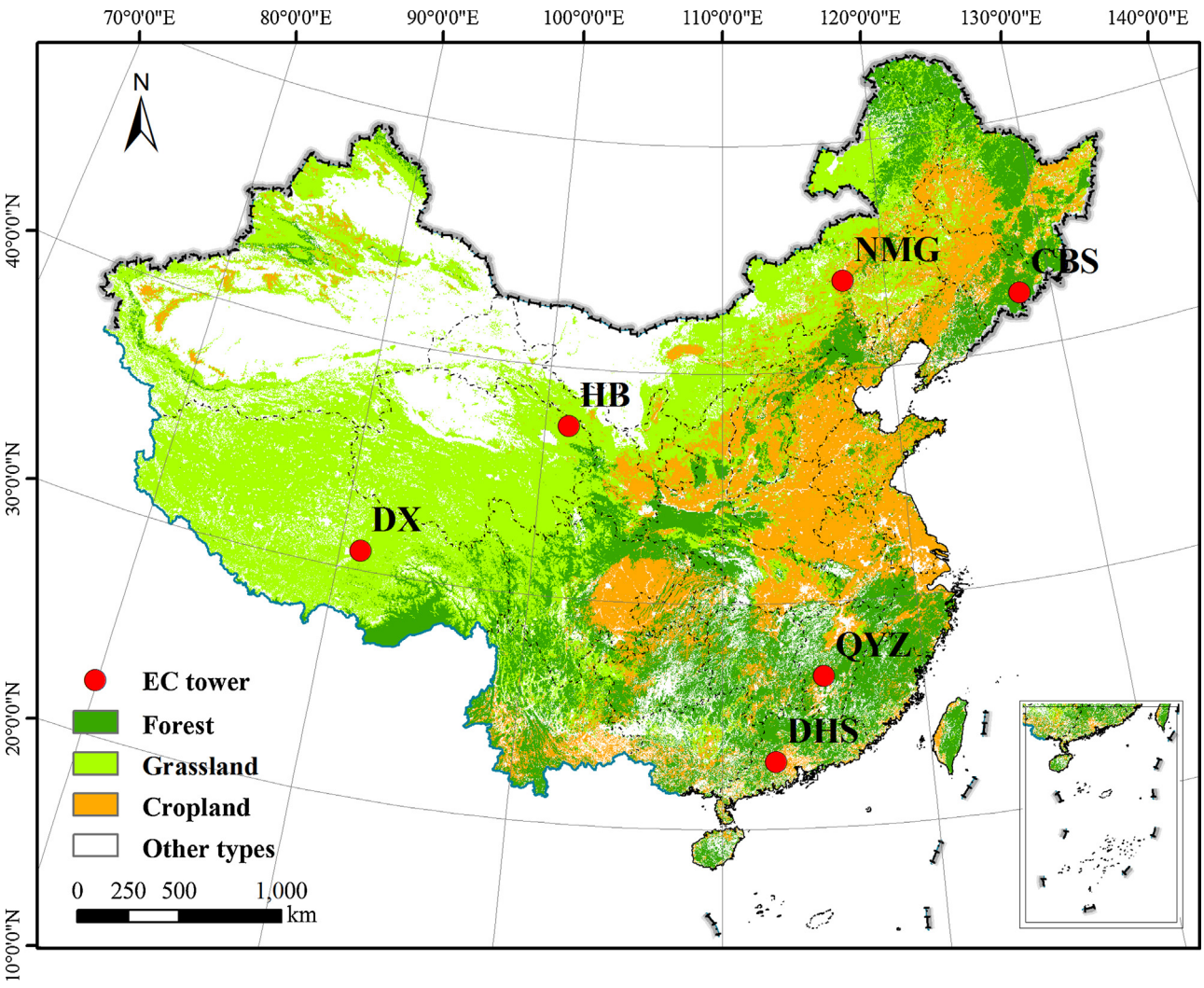

Fig. 1. Distribution of the 7 sites in China in this study. The background was the MODIS land cover map.

Eq. (1). Negative NEE values denote carbon uptake, while positive values denote carbon source.

$$\mathrm{NEE} = \overline{w'\rho_c'(z_r)} + \int_0^{z_r} \frac{\delta\bar{\rho}_c}{\delta t} dz, \quad (1)$$

where the first term on right-hand side of Eq. (1) is the eddy flux for carbon dioxide, and the second term is the CO_2 storage below the height of EC tower observation (z_r); w represents the vertical wind velocity (ms^{-1}), ρ_c represents the CO_2 concentration (in mmol m^{-3}) fluctuations, and primes are the deviations from the time-averaged mean. The overbar indicates a time-averaged mean.

Daily GPP data are partitioned from NEE data measured every 30-min using the eddy covariance technique, which was processed using the same method as Zhang et al. (2011). GPP was calculated employing the following equation:

$$\mathrm{GPP} = \mathrm{Re} - \mathrm{NEE} \quad (2)$$

NEE was obtained directly from the eddy covariance measurement. Ecosystem respiration (Re) of the seven sites was estimated using the Lloyd–Taylor equation (1994) (Fu et al., 2006a; Lloyd and Taylor, 1994; Yu et al., 2008a). The nighttime NEE data under turbulent conditions were used to establish Re-temperature response relationship Eq. (3):

$$\mathrm{Re} = R_{\mathrm{ref}} e^{E_0(1/(T_{\mathrm{ref}}-T_0)-1/(T-T_0))} \quad (3)$$

where R_{ref} represents the ecosystem respiration rate at reference temperature (T_{ref}, 10 °C); E_0 is the parameter that determines the temperature sensitivity of ecosystem respiration, and T_0 is a constant and set as −46.02 °C; T is the air temperature or soil temperature (°C). Eq. (3) was also used to estimate daytime Re.

In order to match the MODIS GPP product, daily measured GPP data were transformed to an 8-day temporal resolution by calculating their arithmetic means. Meanwhile, the daily in situ meteorological measurements, including photosynthetically active radiation (PAR), air temperature (T_a), and vapor pressure deficit (VPD), are employed to drive the LUE model.

Flux measurements in 2003, 2004 and 2005 were used to calibrate the model parameters at all the 7 sites. Flux data measured in 2006 and 2007 were used for model validation at CBS, QYZ, DHS, YC, NMG and HB sites, while flux observation in 2006 was used for model validation at DX site (Table 1).

2.2. MODIS data

We used MOD15A2 (LAI & fPAR) and MOD17A2 products (summation of 8-day GPP, $GPP_{\_MOD}$) from MODIS observations at of each flux site in this study. MODIS ASCII subsets (Collection 5) for all products were obtained from the Oak Ridge National Laboratory's Distributed Active Center (DAAC) website (http://daac.ornl.gov/MODIS/). The MODIS ASCII subsets encompass

Table 1
Site descriptions.

Site (abbreviation)	Location	Elevation (m)	Annual mean temperature (°C)	Vegetation type	Percentages of good quality daytime data (%)	Percentages of good quality nighttime data (%)	References
Changbaishan (CBS)	42°24′ N 128°06′ E	738	3.6	Mixed forest	77.66	40.78	Yu et al. (2006), Zhang et al. (2006b)
Qianyanzhou (QYZ)	26°45′ N 115°04′ E	102	18.6	Evergreen needle leaf forest	81.08	13.14	Wen et al. (2010), Yu et al. (2006, 2008b)
Dinghushan (DHS)	23°10′ N 112°32′ E	300	21	Evergreen broadleaf forest	70.2	24.26	Yu et al. (2006, 2008b), Zhang et al. (2011)
Yucheng (YC)	36°57′ N 116°36′ E	28	13.1	Winter wheat/summer corn	47.08	15.86	Zhang et al. (2008)
Haibei (HB)	37°40′ N 101°20′ E	3293	−1.7	Alpine frigid shrub	77.06	16.64	Fu et al. (2009), Zhang et al. (2008)
Inner Mongolia (NMG)	43°32′ N 116°40′ E	1189	−0.4	Temperate steppe	71.54	27.98	Fu et al. (2006a,b), Hao et al. (2007)
Damxung (DX)	30°51′ N 91°05′ E	4333	1.3	Alpine steppe-meadow	68.14	13.16	Fu et al. (2009), Shi et al. (2006)

7 km × 7 km regions centered on the flux tower. For each variable, we extracted average values for the central 3 km × 3 km within the 7 km × 7 km cutouts to better represent the flux tower footprint, and determined the quality of the value of each pixel within the area using the quality assurance (QA) flags included in the product (Xiao et al., 2008). The bad values of MODIS data were replaced by a simple linear interpolation approach (Zhao et al., 2005).

2.3. CI-LUE model algorithm

We developed a cloudiness index light use efficiency (CI-LUE) model to estimate the GPP on the basis of the MODIS-photosynthesis (MOD17) model algorithm (Running et al., 2000). With maximum light use efficiency in the MOD17 model replacing by the base light use efficiency following the CFLUX model (Turner et al., 2006b), GPP was calculated as:

$$\mathrm{GPP} = \epsilon_{\mathrm{base}} \times \mathrm{PAR} \times \mathrm{fPAR} \times f(T_a) \times f(\mathrm{VPD}) \quad (4)$$

where $\varepsilon_{\mathrm{base}}$ is the base light use efficiency (gC m^{-2} MJ^{-1} APAR), PAR is the incident photosynthetically active radiation (MJ m^{-2} d^{-1}), fPAR is the fraction of PAR absorbed by vegetation canopies, APAR (PAR × fPAR) is the absorbed PAR by vegetation canopy, $f(T_a)$ is the air temperature (T_a) scalar, $f(VPD)$ is the VPD scalar.

As illustrated in Eq. (4), GPP was estimated by the LUE approach which was first proposed by Monteith and Moss (1977) and widely applied for modeling GPP (He et al., 2013; Landsberg and Waring, 1997; Prince and Goward, 1995; Veroustraete et al., 2002; Xiao et al., 2004; Yang et al., 2013; Yuan et al., 2007). T_a scalar and VPD scalar represent limitations of temperature and water on GPP, respectively, which are used to downscale the $\varepsilon_{\mathrm{base}}$ to the actual. A cloudiness index implemented in the CFLUX model was used in our model, since an increase on light use efficiency under overcast conditions at both hourly and daily time steps has been found in previous studies (Kanniah et al., 2013; Rossini et al., 2012; Sakowska et al., 2014; Turner et al., 2003, 2006b). The cloudiness index was calculated as (Turner et al., 2006b):

$$\mathrm{CI} = 1 - {\downarrow}\mathrm{PAR} / {\downarrow}\mathrm{PAR}_{\mathrm{po}} \quad (5)$$

where CI is the cloudiness index, ↓PAR is incident PAR (MJ m^{-2}) from daily tower measurements, $\downarrow\mathrm{PAR}_{\mathrm{po}}$ is potential incident PAR as a derivation of the algorithm proposed by Fu and Rich (1999). With the inputs of digital elevation model (DEM) and specified parameters, the daily potential incident PAR data were calculated as the global radiation or amount of incoming solar insolation (direct and diffuse) at each flux site.

The cloudiness index scalar and base light use efficiency ($\varepsilon_{\mathrm{base}}$) were calculated as (King et al., 2011; Turner et al., 2006b):

$$S_{\mathrm{CI}} = \frac{\mathrm{CI_d} - \mathrm{CI_{min}}}{\mathrm{CI_{max}} - \mathrm{CI_{min}}} \quad (6)$$

$$\epsilon_{\mathrm{base}} = (\epsilon_{\mathrm{max}} - \epsilon_{\mathrm{cs}}) \times S_{\mathrm{CI}} + \epsilon_{\mathrm{cs}} \quad (7)$$

where S_{CI} is cloudiness index scalar varying from 0 on clear days to 1 on fully cloudy days, $\mathrm{CI_d}$ is cloudiness index for the specific day, $\mathrm{CI_{min}}$ is minimum CI, $\mathrm{CI_{max}}$ is maximum CI, $\varepsilon_{\mathrm{max}}$ is maximum LUE, $\varepsilon_{\mathrm{cs}}$ is clear sky LUE. $\varepsilon_{\mathrm{max}}$ is an optimized parameter, and $\varepsilon_{\mathrm{cs}}$ is the value based on the flux tower observation (LUE = GPP/APAR) when $\mathrm{PAR/PAR_{po}}$ approximates 1.0 (King et al., 2011; Turner et al., 2006b). In this study, the exact value of $\varepsilon_{\mathrm{cs}}$ was determined when the absolute value of the difference between $\mathrm{PAR/PAR_{po}}$ and 1.0 reached the minimal one.

We used the VPD and T_a scalar implemented in the MOD17 model (Running et al., 2000):

$$f(\mathrm{VPD}) = \begin{cases} 0 & \mathrm{VPD} \geq \mathrm{VPD_{max}} \\ \dfrac{\mathrm{VPD_{max}} - \mathrm{VPD}}{\mathrm{VPD_{max}} - \mathrm{VPD_{min}}} & \mathrm{VPD_{min}} < \mathrm{VPD} < \mathrm{VPD_{max}} \\ 1 & \mathrm{VPD} \leq \mathrm{VPD_{min}} \end{cases} \quad (8)$$

$$f(T_a) = \begin{cases} 0 & T_a \leq T_{\mathrm{min}} \\ \dfrac{T - T_{\mathrm{min}}}{T_{\mathrm{max}} - T_{\mathrm{min}}} & T_{\mathrm{min}} < T_a < T_{\mathrm{max}} \\ 1 & T_a \geq T_{\mathrm{max}} \end{cases} \quad (9)$$

where $\mathrm{VPD_{max}}$, $\mathrm{VPD_{min}}$, T_{min}, T_{max} are parameters dependent on vegetation types (Table 2). Further details of Eqs. (8) and (9) can be found in Running et al. (2000).

Table 2
Parameters of $\varepsilon_{\mathrm{max}}$, $\mathrm{VPD_{max}}$, $\mathrm{VPD_{min}}$, T_{min} and T_{max} of different plant function types (PFT) in MOD17 model.

Vegetation type[a]	ENF	EBF	MF	Grass	Crop
$\varepsilon_{\mathrm{max}}$ (gC MJ^{-1})	1.008	1.259	1.116	0.604	0.604
T_{max} (°C)	8.31	9.09	8.50	12.02	12.02
T_{min} (°C)	8.00	8.00	8.00	8.00	8.00
$\mathrm{VPD_{max}}$ (kPa)	4.10	4.10	4.10	4.10	4.10
$\mathrm{VPD_{min}}$ (kPa)	0.93	0.93	0.93	0.93	0.93

[a] ENF: evergreen needle leaf forest; EBF: evergreen broadleaf forest; MF: mixed forest.

2.4. Model parameter optimization

We used the differential evolution (DE) algorithm (Price et al., 2005) to derive the parameters of CI-LUE in this study. Differential evolution did not require derivatives of the objective function. It was useful in situations in which the objective function is stochastic, noisy, or difficult to differentiate (Mullen et al., 2011). DE algorithm was an evolutionary technique similar to classic genetic algorithms that was a powerful tool for solving the global optimization problem. One prevalent feature of DE is that it can obtain the global minimum of a sophisticated model fast and with high reliability (Xiao et al., 2011). The algorithm is an evolutionary technique which at each generation transforms a set of parameters vectors, the members of which are more likely to minimize the objective function. The DEoptim package (Mullen et al., 2011) in the R statistically package was implemented in our analysis.

In our model, the calibrated parameter (ε_{max}) was allowed to vary in a certain range in order to get the best estimation. The ranges of ε_{max} were set to 0–12 gC MJ^{-1} at forest sites (CBS, QYZ and DHS), 0–4 gC MJ^{-1} at cropland site (YC) and 0–2 gC MJ^{-1} at grassland sites (HB, NMG and DX) (Zhang et al., 2006a, 2008).

2.5. Model validation and comparisons

The determination coefficient (R^2) and root mean square error (RMSE) were used to evaluate the model performance. In addition to validation against measured GPP, the capacity of the CI-LUE model to simulate GPP was compared with GPP simulated by MOD17 model driven by in situ meteorological measurements ($GPP_{\_17}$), MODIS GPP products ($GPP_{\_MOD}$), the VPM algorithm (Xiao et al., 2004), and the TEC model proposed by Yan et al. (2015). The VPM model employed climate data, MODIS Land Surface Water Index (LSWI) and EVI to calculate 8-day GPP. The TEC GPP model integrated MODIS fPAR and climate measurements to simulate GPP at the monthly temporal scale, with the incorporation of a new water stress scalar defined as the ratio of actual evapotranspiration to potential evaporation derived from a precipitation-driven evapotranspiration model (Yan et al., 2012).

3. Results

3.1. Parameter calibration

The calibrated ε_{max} of LUE model was shown in Table 3. All the parameters converged within prior bounds for all sites, and exhibited an extensive variability across ecosystem types. For example, optimized ε_{max} varied substantially among different ecosystems. The optimized ε_{max} of mixed forest (CBS) was higher than those of the other sites, while those of grassland sites (NMG, HB and DX) were lowest among the three ecosystem types. The estimated value of E_0 came to the maximum in a subtropical plantation ecosystem (QYZ), and fell to the bottom at the HB grassland site. Meanwhile, the calibrated ε_{max} in our model differed considerably within the ecosystem type. For example, the ε_{max} of three forest ecosystems was 3.867 (CBS), 2.676 (QYZ) and 2.087 (DHS) gC MJ^{-1}, respectively. The ε_{max} at HB site was higher than the other two grassland sites (NMG and DX). This suggested more detailed parameterization scheme of ε_{max} was required in regional flux simulations with LUE models.

Table 3
Calibrated maximum light use efficiency (ε_{max}) for each flux observation site.

Site	CBS	QYZ	DHS	NMG	HB	DX	YC
ε_{max} (gC MJ^{-1})	3.867	2.676	2.087	0.838	1.610	0.48	2.453

3.2. Validation of daily GPP

Fig. 2 exhibited the comparison of daily tower-measured ($GPP_{\_obs}$) with GPP simulated by CI-LUE model ($GPP_{\_simu}$). On the whole, the $GPP_{\_simu}$ showed similar seasonal dynamics with $GPP_{\_obs}$. Except that the seasonal variations at DHS site were quite small; both the simulated and observed GPP demonstrated distinguishable seasonality in three kinds of ecosystem. At two forest sites (CBS and QYZ), GPP values were low in spring and winter, while those were high in summer and autumn. In consequence of two rotations (winter wheat and summer maize), two peaks of GPP in May and August were observed at the YC site, respectively, in which growth peaks of winter wheat and summer maize were occurred.

Basically, the $GPP_{\_simu}$ was in good consistency with $GPP_{\_obs}$ in the validation years at each site. The R^2 value of $GPP_{\_simu}$ against $GPP_{\_obs}$ ranged from 0.58 (at DHS) to 0.95 (at HB). RMSE was in the range from 0.4 gC m^{-2} d^{-1} (at NMG) to 2.13 gC m^{-2} d^{-1}(at YC). With higher R^2 values and lower RMSE values, the $GPP_{\_simu}$ was in better conformity to $GPP_{\_obs}$ at grassland sites than at forest and cropland sites. GPP values were overestimated at QYZ, HB and DX, while those were underestimated at CBS, DHS, NMG and YC sites. Among sites, the R^2 value at DHS site was lower than what at other sites. This may be attributed to the large difference of soil water content between the calibration years and absence of soil water content scalar in the GPP simulation (He et al., 2013).

3.3. Comparisons of GPP derived from multiple models

Fig. 3 illustrated the seasonal variations of 8-day observed GPP ($GPP_{\_obs}$), 8-day CI-LUE model simulated GPP ($GPP_{\_simu8d}$) and MODIS GPP products ($GPP_{\_MOD}$) at seven typical sites in the validation years. $GPP_{\_MOD}$ was lower than $GPP_{\_obs}$ at all sites except the NMG and HB sites. This was attributable to the lower default ε_{max} values used to produce MODIS GPP product. Compared with $GPP_{\_MOD}$, closer agreement was found between $GPP_{\_simu8d}$ and $GPP_{\_obs}$.

Fig. 4 demonstrated the comparisons of 8-day $GPP_{\_obs}$ with $GPP_{\_MOD}$ and $GPP_{\_simu8d}$ in the validation years at the seven sites. Generally, with higher R^2 and lower RMSE values, $GPP_{\_simu8d}$ matched better with $GPP_{\_obs}$ in comparison with $GPP_{\_MOD}$. To an illustration, the R^2 value of $GPP_{\_simu8d}$ against $GPP_{\_obs}$ at DHS was 0.61, much higher than the corresponding value of $GPP_{\_MOD}$ which is 0.17. Another, the RMSE value of $GPP_{\_simu8d}$ at YC site was 17.83 gC m^{-2} (8d)$^{-1}$, while that of $GPP_{\_MOD}$ was 35.66 gC m^{-2} (8d)$^{-1}$. At certain sites (e.g. CBS, HB), despite that the R^2 values of $GPP_{\_simu8d}$ against $GPP_{\_obs}$ were less than or equal to the corresponding value of $GPP_{\_MOD}$, the RMSE values of $GPP_{\_MOD}$ were much higher than those of $GPP_{\_simu8d}$.

In brief, the 8-day GPP calculated by our light use efficiency model (CI-LUE) performed much better than 8-day MODIS GPP product at most sites in China, which were comprised of forest, grassland and cropland ecosystems. The most important improvement achieved by the CI-LUE model was at the DHS site, and R^2 increased from 0.17 to 0.61 despite the value of RMSE which increased by 0.2 gC m^{-2} (8d)$^{-1}$. Followed by the YC site, the CI-LUE model outperformed MODIS GPP product, with the R^2 increased from 0.76 to 0.8 and RMSE decreased from 35.66 to 17.83 gC m^{-2} (8d)$^{-1}$. The comparison above indicated both the potential of improvement on MODIS GPP products and better capturing the seasonal dynamics of flux measurements through the implementation of CI-LUE model.

Additionally, simulation performance comparisons of 8-day VPM model GPP (GPP_V) and monthly TEC model GPP (GPP_T) with CI-LUE model ($GPP_{\_simu}$) at correspondingly time scales were shown in Table 4. In general, both the VPM model and TEC model

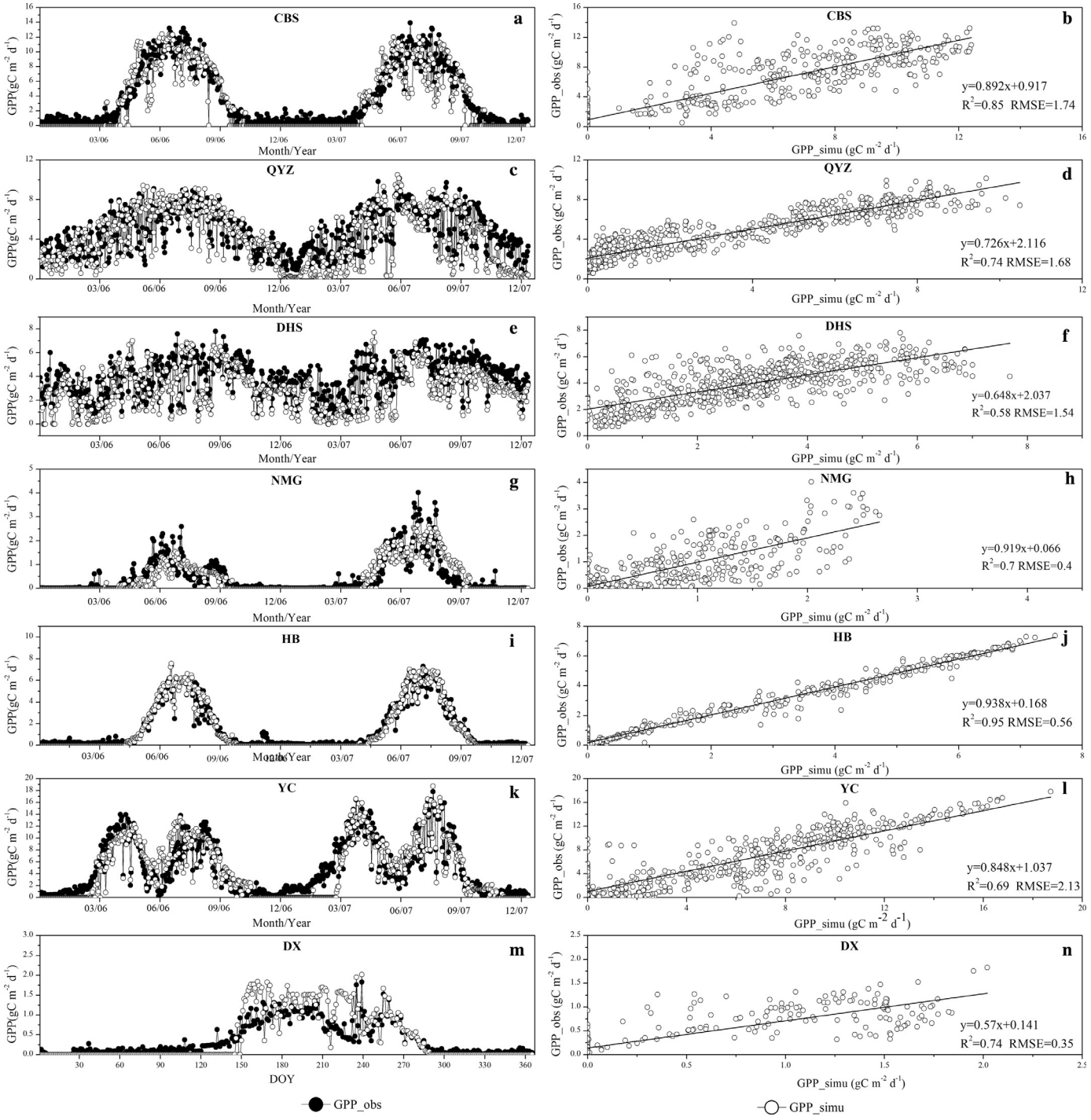

Fig. 2. Seasonal variations of daily tower-measured GPP (GPP_{obs}) and GPP simulated (GPP_{simu}) by our LUE model in the validation years at CBS (a, b), QYZ (c, d), DHS (e, f), NMG (g, h), HB (i, j), YC (k, l) and DX (m, n). Root mean square error (RMSE) was in unit of gC m^{-2} d^{-1}.

were efficient in capturing the observed GPP dynamics at 8-day and monthly time scale, respectively. The R^2 values of GPP_V ranged from 0.84 (at DX) to 0.92 (at HB), while the RMSE values varied from 1.96 (at DX) to 13.6 (at CBS) gC m^{-2} $(8d)^{-1}$. And R^2 values of TEC model GPP were in the range from 0.62 (at NMG) to 0.94 (at CBS), while the RMSE values ranged from 18.53 (at HB) to 74.74 (at YC) gC m^{-2} mon^{-1}. Another, the 8-day GPP simulated by CI-LUE model (GPP_{simu8d}) outperformed the VPM model in tracking the observed GPP variation trends at one forest site (CBS) and one grassland site (HB) with higher R^2 values and lower RMSE values. And the VPM model performed better than those of CI-LUE model in predicting the seasonal dynamics of GPP at two grassland sites (NMG and DX). According to the previous studies, VPM model had explicitly demonstrated the great potential of simulating GPP of grassland ecosystems in China (Li et al., 2007; Liu et al., 2012; Wu et al., 2008a,b; Yan et al., 2009). Absence of soil moisture scalar in CI-LUE model may be responsible for the less accurate prediction at the grassland sites, which were water-driven ecosystems (Ogutu and Dash, 2013). Therefore, constraint of soil water content on GPP are expected in the further model research. At the monthly time scale, both GPP_{mon} and GPP_T were in good agreement with in situ flux measurements (Table 4). The R^2 values of GPP_T against flux

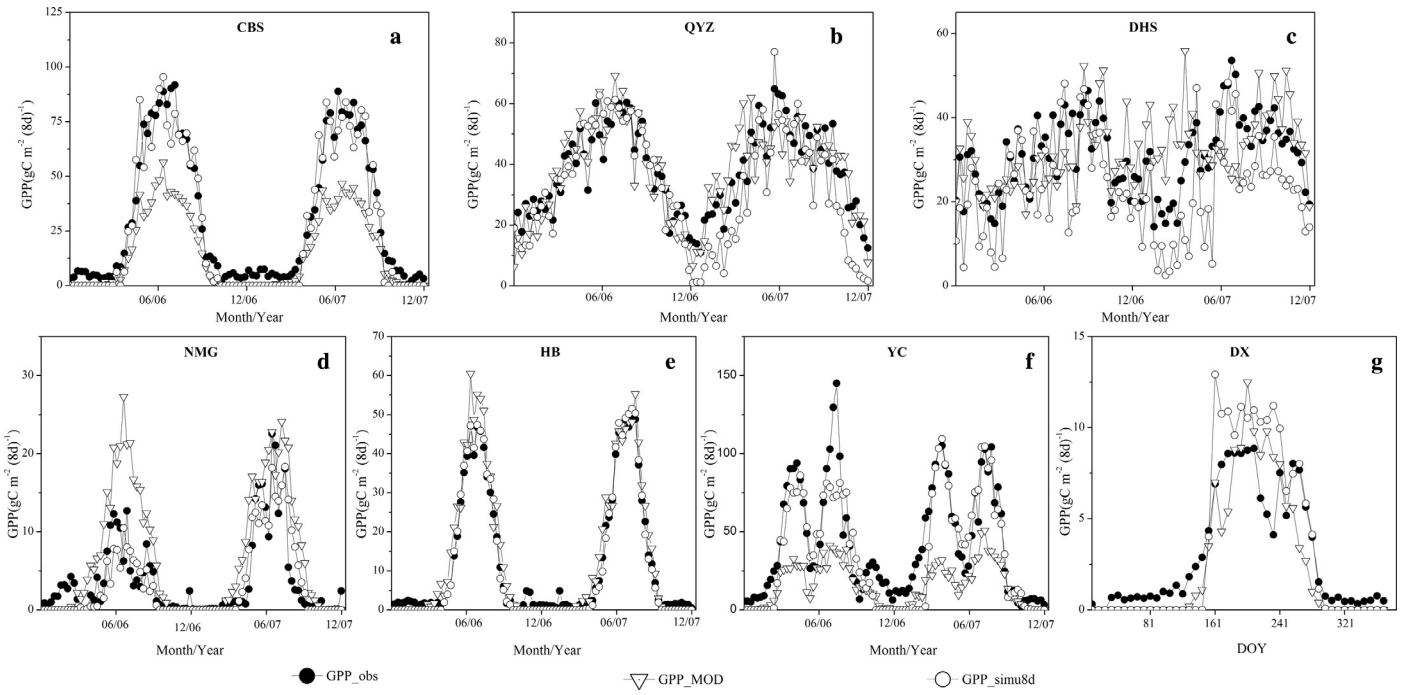

Fig. 3. Seasonal variations of 8-day GPP_{obs}, 8-day GPP_{MOD} and 8-day GPP_{simu8d} at multi-sites in the validation years (GPP_{simu8d} was the 8-day GPP calculated with the CI-LUE model. GPP_{MOD} was the 8-day MODIS GPP products).

observation ranged from 0.62 (NMG) to 0.94 (CBS), while those of GPP_{mon} were in the range from 0.83 (NMG and YC) to 0.99 (HB). At the CBS site, the CI-LUE model performed marginally better than that of TEC model as indicated by a small increase on R^2 values (0.94–0.95) but a slight increment of RMSE values by 1.47 gC m^{-2} mon^{-1}. The performance of our LUE model was obviously better than the TEC model in predicting the monthly GPP dynamics at the other six sites as indicated by higher or equal R^2 values and large reductions on RMSE values. Especially, CI-LUE model greatly improved the prediction of GPP in comparison with TEC model at DHS site, as the R^2 value increased by 0.14 and RMSE value decreased by 39.99 gC m^{-2} mon^{-1}. This great alleviation of

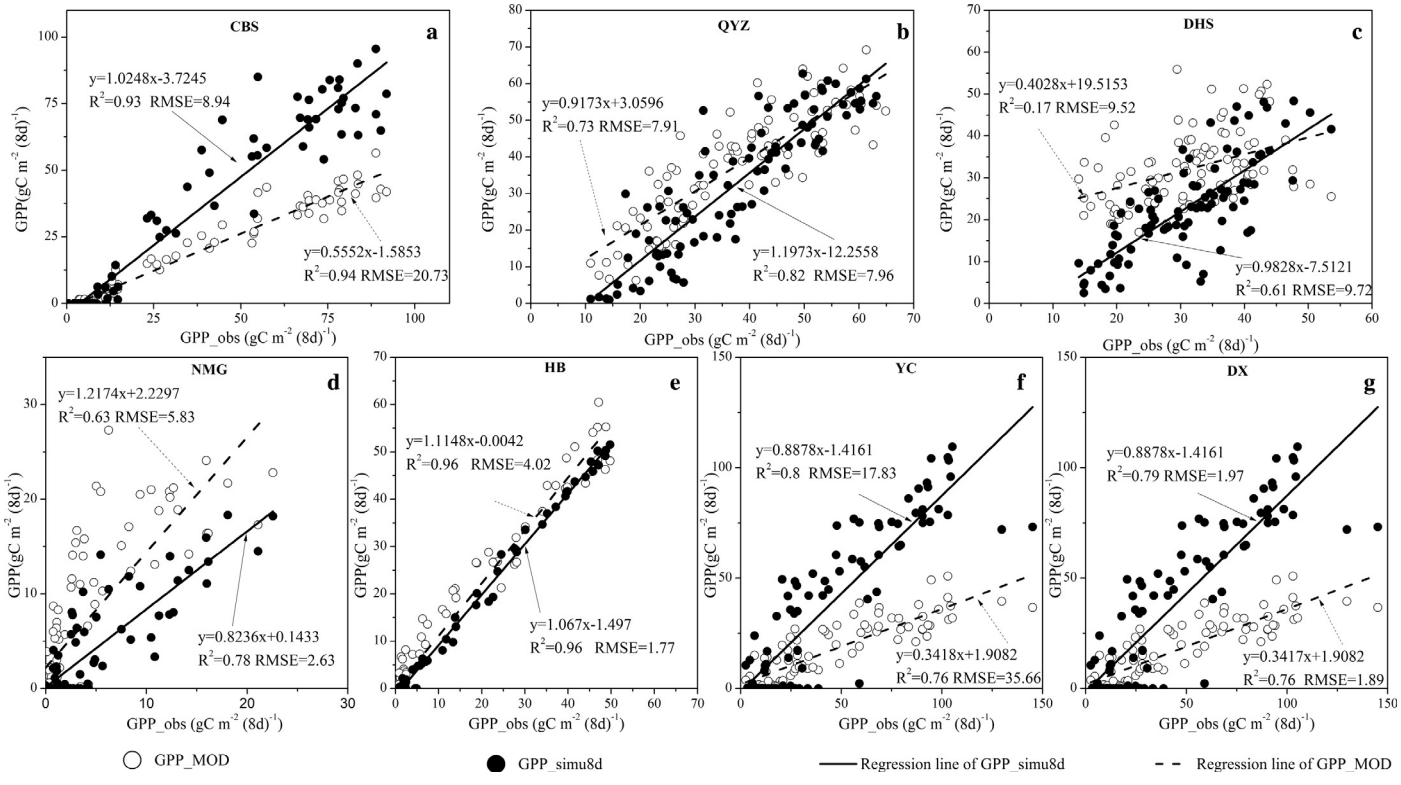

Fig. 4. Comparisons of 8-day tower-measured GPP (GPP_{obs}), 8-day GPP_{simu8d} and GPP_{MOD} at seven sites in the validation years.

Table 4
Statistics for the comparisons of 8-day $GPP_{\_simu8d}$, monthly GPP calculated by our CI-LUE model ($GPP_{\_mon}$), GPP calculated by VPM model (GPP_V) and GPP calculated by TEC model (GPP_T) with the tower-measured GPP ($GPP_{\_obs}$) of seven typical sites at correspondingly time scale in the validation years.

Site	R^2				RMSE ($gC\,m^{-2}(8d)^{-1}$)		RMSE ($gC\,m^{-2}\,mon^{-1}$)	
	$GPP_{\_simu8d}$	GPP_V	$GPP_{\_mon}$	GPP_T	$GPP_{\_simu8d}$	GPP_V	$GPP_{\_mon}$	GPP_T
CBS	0.93	0.85	0.95	0.94	8.94	13.6	30.24	28.77
QYZ	0.82	–	0.89	0.89	7.96	–	32.20	35.05
DHS	0.61	–	0.85	0.71	9.72	–	33.27	73.26
NMG	0.78	0.85	0.83	0.62	2.63	2.89	7.83	23.74
HB	0.96	0.92	0.99	0.94	1.77	5.38	5.41	18.53
DX	0.79	0.84	0.93	0.87	1.97	1.96	7.04	19.26
YC	0.8	–	0.83	0.75	17.83	–	57.12	74.74

'–' Data not available.

CI-LUE GPP simulations at the DHS site was also found in the comparison of $GPP_{\_simu8d}$ with $GPP_{\_MOD}$ above (Fig. 4c).

Overall, at 8-day time scale, the CI-LUE model had the best agreement with in situ GPP measurements at the mixed forest site ($R^2 = 0.95$, CBS) followed by the MODIS GPP products ($R^2 = 0.94$, CBS) and lastly VPM model ($R^2 = 0.85$, CBS). Instead, the VPM model outperformed in predicting GPP at the steppe site (NMG) and the meadow site (DX) followed by the CI-LUE model and lastly the MODIS GPP products, with an exception that CI-LUE model performed best at the shrub site (HB). For the cropland site (YC), the CI-LUE model performed better than MODIS GPP products as demonstrated by a higher R^2 value and a much lower RMSE value. At the monthly time scale, the TEC model could capture the GPP seasonal dynamics at seven flux sites (Fig. 5). Compared with observed GPP and CI-LUE simulated GPP, ecosystem GPP were overestimated by TEC model at two forest sites (QYZ and DHS) and two grassland sites (NMG and DX). And the TEC model underestimated ecosystem GPP at the steppe site (HB) and cropland site (YC). The CI-LUE model performed much better than those of TEC model in tracking the GPP dynamics at the seven sites.

3.4. Ecosystem light use efficiency enhanced by the diffuse radiation

Here the variation of mean LUE in different ranges of CI was used to illustrate how the terrestrial ecosystem carbon sequestration capacity varied with the fraction of diffuse radiation across different types of ecosystems. Fig. 6 showed the changes of daily canopy light use efficiency (LUE_c = GPP/PAR) observed at towers in the growing seasons of one calibration year (May to September, 2003). Apparently, the observed LUE_c exhibited obviously increasing trends with the increasing cloudiness index at all sites. The increasing rates were greatest at forests site (CBS, 3.467 gC MJ^{-1}), intermediate at cropland site (YC, 2.744 gC MJ^{-1}), and lowest at grassland site (NMG, 0.223 gC MJ^{-1}). Those were consistent with the expectation that canopy LUE could be enhanced by the diffuse components of solar radiation compared to direct radiation

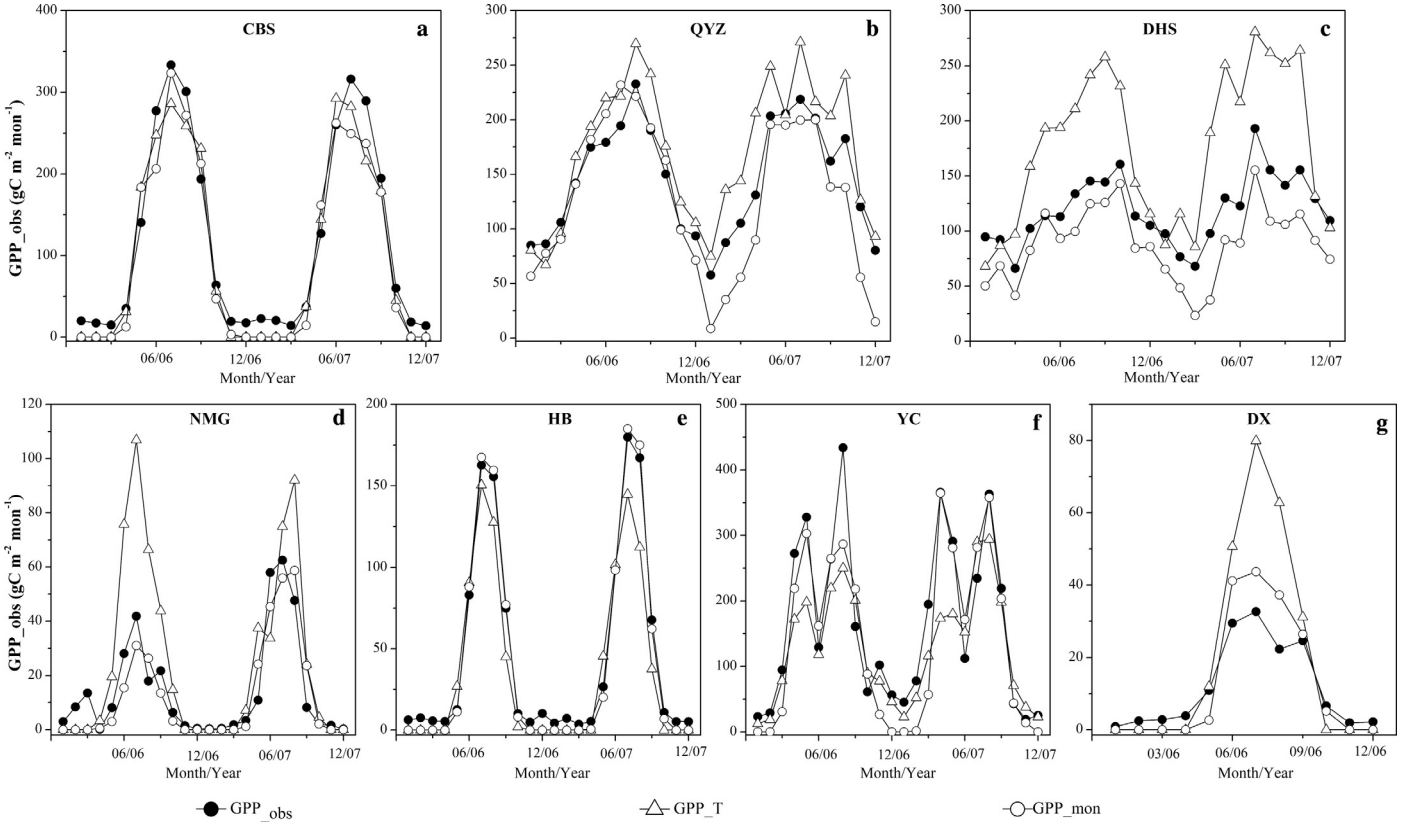

Fig. 5. Seasonal dynamics of monthly $GPP_{\_obs}$, monthly $GPP_{\_T}$ and monthly $GPP_{\_mon}$ at multi-sites in the validation years. ($GPP_{\_mon}$ was the monthly GPP calculated with the CI-LUE model. $GPP_{\_T}$ was the monthly GPP simulated by the TEC model).

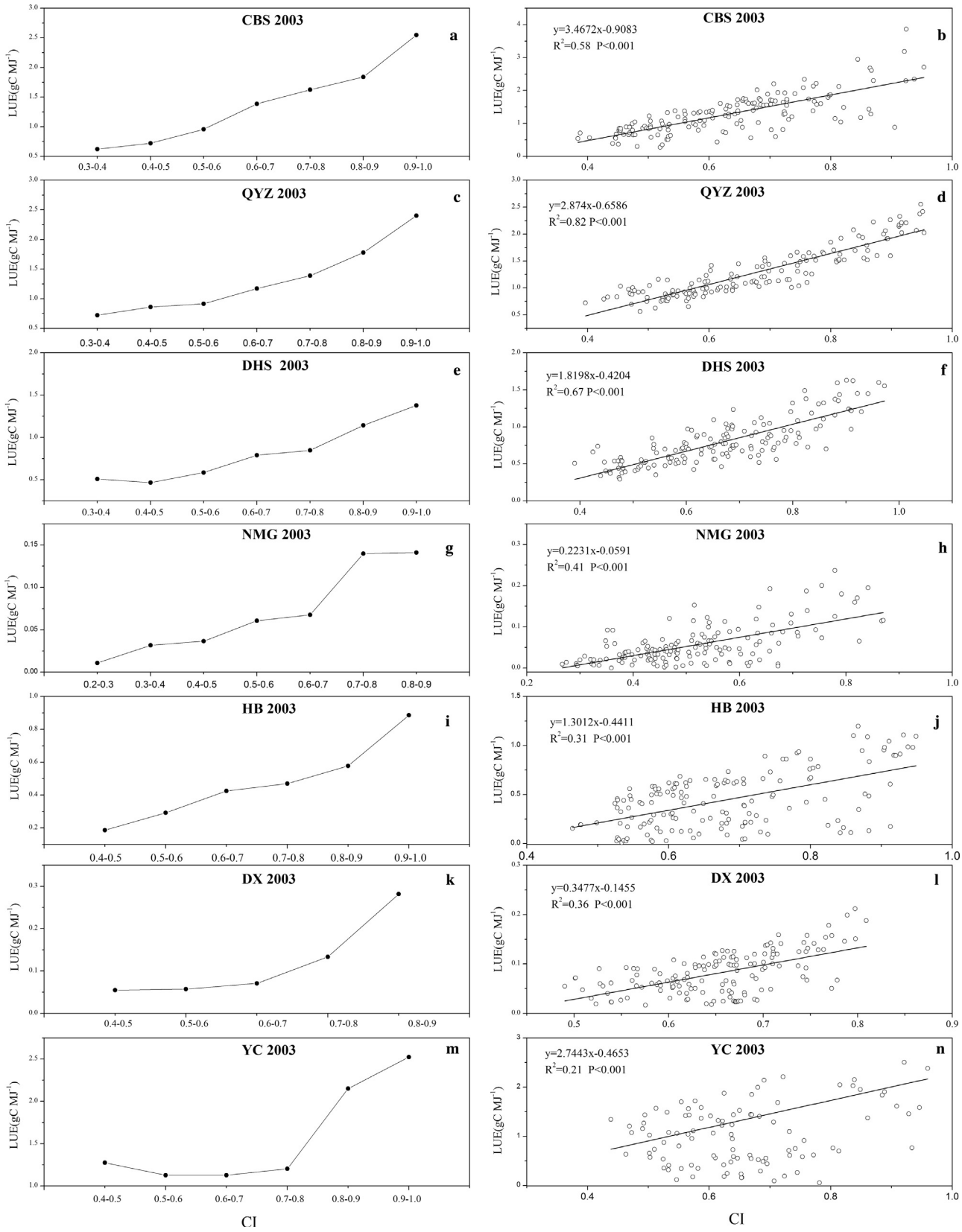

Fig. 6. Dependence of canopy light use efficiency (LUEc = GPP/PAR) on cloudiness index (CI) averaged over 0.1bins of CI in the growing seasons (May to September) of one calibration year (2003).

(Farquhar and Roderick, 2003; Gu et al., 2002, 2003). In addition, differences in canopy structure density across different ecosystem types were reported to contribute to the increasing rate sensitivity of LUE to fraction of diffuse radiation (Kanniah et al., 2012; Zhang et al., 2011), due to its effective penetration to the lower depths of canopy (Ren et al., 2013; Urban et al., 2007). For the forest sites,

Table 5
Statistics for the comparisons of 8-day GPP calculated with CI-LUE model ($GPP_{\_simu8d}$) and 8-day GPP calculated using MOD17 model ($GPP_{\_17}$) driven by in situ tower-measured meteorological data with the tower-measured GPP at the 7 study sites in the validation years.

Site	R^2		RMSE ($gC\,m^{-2}(8d)^{-1}$)	
	$GPP_{\_simu8d}$	$GPP_{\_17}$	$GPP_{\_simu8d}$	$GPP_{\_17}$
CBS	0.93	0.93	8.94	15.68
QYZ	0.82	0.74	7.96	7.90
DHS	0.61	0.49	9.72	9.50
NMG	0.78	0.70	2.63	2.82
HB	0.96	0.96	1.77	1.93
DX	0.79	0.78	1.97	2.06
YC	0.80	0.79	17.83	20.02

significantly increasing rates of LUE existed among different forest sites, which showed obviously decreasing trends with decreasing latitudes (Huang et al., 2014). The growing season length of temperate mixed forest in Changbai Mountain (CBS) was much less than those of two subtropical forest sites (QYZ and DHS), thus a higher LUE can compensate for the ecosystem carbon sink capacity (Yu et al., 2013). Also, the higher sensitivity of LUE increasing rate to diffuse radiation might be ascribed to the fact that the average annual diffuse radiation of China in the last three decades was lower in the north and higher in the south (Ren et al., 2013). At the grassland sites, the increasing rate of LUE enhanced by diffuse radiation ($0.223\ gC\ MJ^{-1}$) was much less than the other two grassland sites (HB and DX). That was partly because the penetration of solar radiation through the canopy of the semi-arid steppe at NMG could be greater than those at other two grassland sites (HB and DX), and the leaf area index (LAI) of those two grassland sites was higher than what at NMG site (Zhang et al., 2011). At the cropland site (YC), the correlation relationship between CI and LUE of growing season was less significant than those in forest sites and grassland sites, which was partly due to the field managements (Li et al., 2006).

4. Discussion

4.1. Capacity to simulate GPP under cloudy days

The comparisons of GPP estimated using CI-LUE model ($GPP_{\_simu8d}$) and MOD17 model ($GPP_{\_17}$) driven by in situ tower-measured meteorological data showed that the CI-LUE model greatly improved the GPP modeling performance under cloudy days (Table 5). In order to investigate the degree, at which the GPP simulation accuracy change with the fraction of diffuse radiation (CI), absolute differences between simulated and observed GPP were binned according to cloudiness index for the validation years (Fig. 7). When CI was above 0.6, the CI-LUE model greatly alleviated the sensitivity of estimated GPP to cloudy conditions, which was indicated by the less underestimation of GPP subject to the more diffuse radiation and enhanced LUE. It has been proved that LUE of the entire canopy could keep in consistency with the increase in the fraction of diffuse radiation, which led to an increase in the illumination free from photo-saturation received by the canopy (Mercado et al., 2009; Oliphant et al., 2011; Zhang et al., 2011). Under cloudy skies (higher CI values), the sunlit leaves often resulted in low LUE induced by light saturated, while the shaded leaves with high LUE were subject to low exposure to the incoming radiation. Under cloudy skies, despite lower total solar radiation and direct radiation received by the canopy, higher portion of diffuse radiation produced a more uniform distributed irradiance of the canopy and resulted in a smaller fraction of canopy light saturated (He et al., 2013; Mercado et al., 2009; Zhang et al., 2011). Therefore, the photosynthesis and

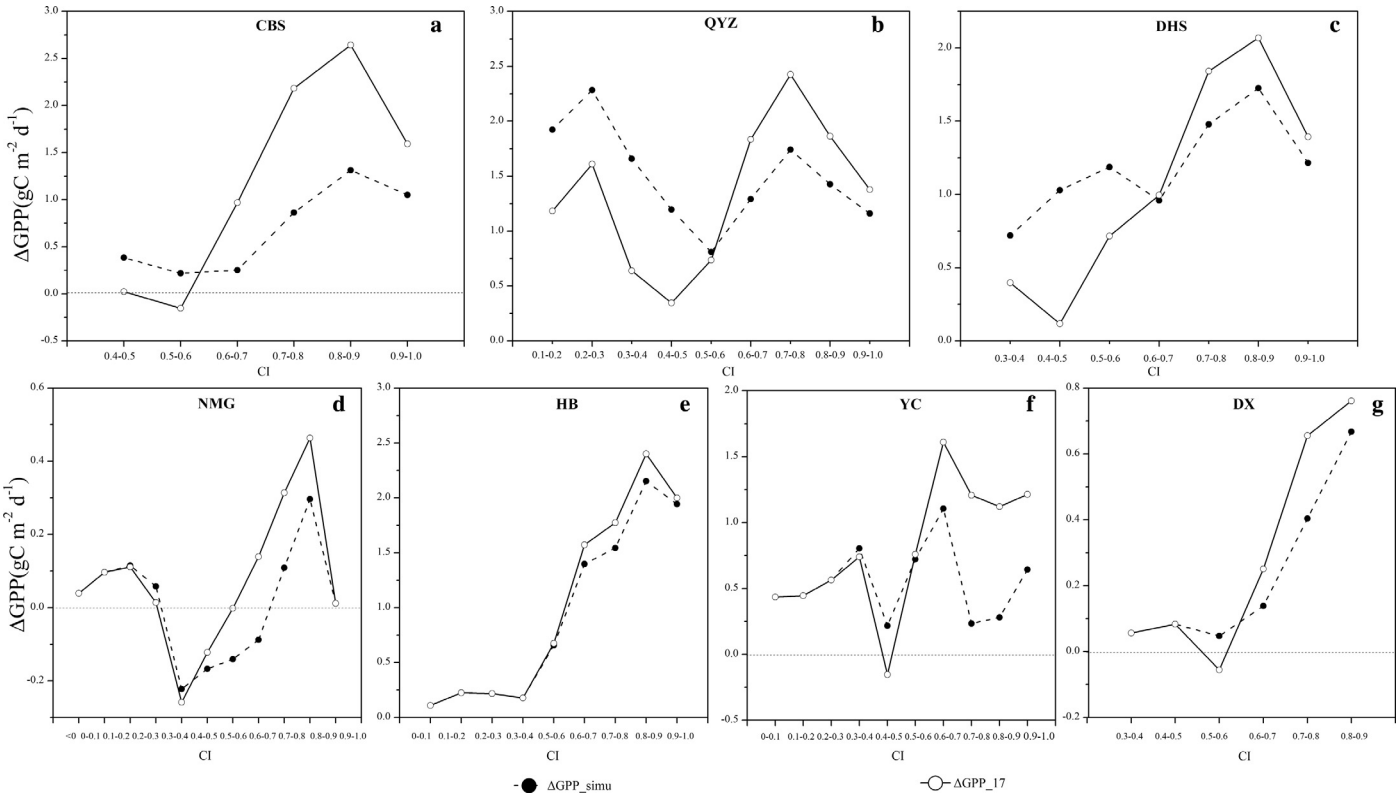

Fig. 7. Dependence of the average absolute errors of GPP estimated using calibrated parameters with cloudiness index (CI) at the 7 study sites in the validation years ($\Delta GPP_{\_simu} = GPP_{\_obs} - GPP_{\_simu8d}$, $\Delta GPP_{\_17} = GPP_{\_obs} - GPP_{\_17}$, positive values mean the underestimation of GPP by models, vice versa).

LUE of the canopy in cloudy skies were significantly enhanced than those in clear skies (Farquhar and Roderick, 2003; Gu et al., 2002; Mercado et al., 2009; Yuan et al., 2014). Meanwhile, it was noted that the absolute values of $\Delta GPP_{\_simu}$ were more than those of $\Delta GPP_{\_17}$ at some sites when the values of CI were small. For instance, at CBS site, the percentages of days in the first bin ($0.4 < CI < 0.5$) were 12.1%. 14.8 percentages of CI were less than 0.5 at QYZ site, while 17.8 percentages of CI were less than 0.6 at DHS site. That was verified by the sensitivity of LUE increasing rate to CI in 3 forest sites (Fig. 6). For three grassland sites and one cropland site, the GPP calculated using CI-LUE model were generally of smaller underestimation than the MOD17 model. Overall, the GPP underestimations were significantly reduced with the CI-LUE model when more diffuse radiation was received by the vegetation canopy (Table 5).

4.2. Application of the CI-LUE model at regional scale

The CI-LUE model can potentially be used in regional GPP estimation. Despite the study that effect of cloudiness change on ecosystem LUE and water use efficiency was detected by the clearness index (Zhang et al., 2011), it was difficult to incorporate the clearness index into LUE model for regional GPP estimates due to the specification of the highest interval of solar elevation angle in each grid. In our CI-LUE model, the model parameter (CI) was the key factor to regulate the enhancement on ecosystem LUE by diffuse radiation under cloudy days. With the simple inputs of regional digital elevation model (DEM) data and readily available parameters, the $\downarrow PAR_{po}$ can be calculated as the global solar radiation at daily time scale in each grid. Using the regional CI, meteorological measurements and MODIS fPAR data, ecosystem GPP was reproduced regionally.

4.3. Uncertainty

The averaged R^2 of daily GPP simulation derived from CI-LUE model in the validation years across the 7 sites were 0.75. The best performance of CI-LUE model occurred in mixed forest ecosystem (at CBS site) was partly because that the canopy coverage of forest canopy was denser than other ecosystem types, LUE was sensitive to the fraction variation of diffuse radiation in incoming solar radiation reflected by difference in the transfer of direct and diffuse light beams within the canopy (He et al., 2013). Nevertheless, the CI-LUE GPP prediction was less correlated with flux measurements at other forest sites (QYZ and DHS) in comparison with simulated GPP by CI-LUE model at CBS site. This could result from the capacity of MODIS fPAR products to capture the seasonality variation of vegetation greenness and photosynthesis (Ogutu and Dash, 2013). Obviously, it was reported that MODIS fPAR products were less sensitive to the shifts of vegetation growth in evergreen forests in contrast with deciduous forest (Ogutu and Dash, 2013). It has been proved that VPD did not track the impact of soil moisture on productivity adequately (Coops et al., 2007; Kanniah et al., 2009; Leuning et al., 2005). Instead, a water stress factor encompassing land surface water index was employed in the VPM model, which led to its better performance than other LUE models at grassland sites driven by water. For cropland sites, evidences showed MODIS GPP products ($GPP_{\_MOD}$) tended to underestimate GPP of highly productive sites such as cropland ecosystems (Chen et al., 2011; Turner et al., 2006a). This was in consistency with the GPP predictions of CI-LUE model as well as MOD17 model, of which MODIS GPP products highly underestimated the flux measurements (slope = 0.341). The GPP underestimation at YC site in our study was mainly due to the low prescribed maximum LUE term, and possible mean LUE for this ecosystem can reach 2.80 gC MJ^{-1} (Chen et al., 2011; Garbulsky et al., 2010).

5. Conclusion

The CI-LUE model was developed in this study to predict the GPP at 7 typical ecosystem sites, based on the CFLUX model and MOD17 model. A cloudiness index to bring up the ε_{max} under overcast condition was employed in the CI-LUE model. Results indicated that (1) the CI-LUE model captured the seasonal dynamics of daily GPP well with the R^2 values ranging from 0.58 to 0.95; (2) estimated parameter values of maximum LUE (ε_{max}) varied substantially across ecosystem types as well as within ecosystem type; (3) significant increase of canopy LUE with the increase in fraction of diffuse radiation and great alleviation of GPP underestimation under cloudy skies using CI-LUE model were found at all the seven sites; (4) the CI-LUE model outperformed MOD17 model and TEC model in GPP prediction, especially at two subtropical evergreen forest sites in southern China (QYZ and DHS), while the VPM model prediction was in better agreement with observed GPP than that of CI-LUE model at two grassland sites (NMG and DX).

Further improvements on the CI-LUE model are still needed, due to the absence of soil moisture scalar from the GPP prediction and difficulty in estimation for the shifts of soil carbon storage. As soil moisture and VPD directly affect photosynthesis, more GPP models explicitly consider the effect of soil moisture as well as temperature. The effect of water stress on ecosystem photosynthesis may be the most uncertain factor in current LUE GPP models (Yan et al., 2015). Also, model validation needs flux measurements from more sites encompassing various ecosystem types to test the applicability and accuracy, which can lay foundation for the carbon flux upscaling.

Acknowledgements

This study was supported by the CAS for Strategic Priority Research Program (Grant No. XDA05050602), the Key Project in the National Science & Technology Pillar Program of China (Grant No. 2013BAC03B00), the National Natural Science Foundation of China (Grant No. 31070438) and Science and Technology Program of Hebei Province (No. 14293703D).

References

Alton, P.B., North, P.R., Los, S.O., 2007. The impact of diffuse sunlight on canopy light-use efficiency, gross photosynthetic product and net ecosystem exchange in three forest biomes. Glob. Change Biol. 13, 776–787.

Baldocchi, D., Falge, E., Gu, L.H., Olson, R., Hollinger, D., Running, S., Anthoni, P., Bernhofer, C., Davis, K., Evans, R., Fuentes, J., Goldstein, A., Katul, G., Law, B., Lee, X.H., Malhi, Y., Meyers, T., Munger, W., Oechel, W., Paw U, K.T., Pilegaard, K., Schmid, H.P., Valentini, R., Verma, S., Vesala, T., Wilson, K., Wofsy, S., 2001. FLUXNET: a new tool to study the temporal and spatial variability of ecosystem-scale carbon dioxide, water vapor, and energy flux densities. Bull. Am. Meteorol. Soc. 82, 2415–2434.

Cai, W.W., Yuan, W.P., Liang, S.L., Zhang, X.T., Dong, W.J., Xia, J.Z., Fu, Y., Chen, Y., Liu, D., Zhang, Q., 2014. Improved estimations of gross primary production using satellite-derived photosynthetically active radiation. J. Geophys. Res.: Biogeosci. 119, 110–123.

Chen, J.M., Liu, J., Cihlar, J., Goulden, M.L., 1999. Daily canopy photosynthesis model through temporal and spatial scaling for remote sensing applications. Ecol. Model. 124, 99–119.

Chen, T.X., van der Werf, G.R., Dolman, A.J., Groenendijk, M., 2011. Evaluation of cropland maximum light use efficiency using eddy flux measurements in North America and Europe. Geophys. Res. Lett. 38 .

Coops, N.C., Jassal, R.S., Leuning, R., Black, A.T., Morgenstern, K., 2007. Incorporation of a soil water modifier into MODIS predictions of temperate Douglas-fir gross primary productivity: initial model development. Agric. For. Meteorol. 147, 99–109.

Falge, E., Baldocchi, D., Olson, R., Anthoni, P., Aubinet, M., Bernhofer, C., Burba, G., Ceulemans, R., Clement, R., Dolman, H., Granier, A., Gross, P., Grunwald, T., Hollinger, D., Jensen, N.O., Katul, G., Keronen, P., Kowalski, A., Lai, C.T., Law, B.E., Meyers, T., Moncrieff, H., Moors, E., Munger, J.W., Pilegaard, K., Rannik, U., Rebmann, C., Suyker, A., Tenhunen, J., Tu, K., Verma, S., Vesala, T., Wilson, K., Wofsy, S., 2001. Gap filling strategies for defensible annual sums of net ecosystem exchange. Agric. For. Meteorol. 107, 43–69.

Farquhar, G.D., Roderick, M.L., 2003. Atmospheric science: Pinatubo, diffuse light, and the carbon cycle. Science 299, 1997–1998.
Farquhar, G.D., von Caemmerer, S., Berry, J.A., 1980. A biochemical model of photosynthetic CO_2 assimilation in leaves of C3 species. Planta 149, 78–90.
Feddema, J.J., Oleson, K.W., Bonan, G.B., Mearns, L.O., Buja, L.E., Meehl, G.A., Washington, W.M., 2005. The importance of land-cover change in simulating future climates. Science 310, 1674–1678.
Fu, P., Rich, P.M., 1999. Design and implementation of the Solar Analyst: an ArcView extension for modeling solar radiation at landscape scales. In: Proceedings of the 19th Annual ESRI User Conference, San Diego, USA.
Fu, Y., Zheng, Z., Yu, G., Hu, Z., Sun, X., Shi, P., Wang, Y., Zhao, X., 2009. Environmental influences on carbon dioxide fluxes over three grassland ecosystems in China. Biogeosciences 6, 2879–2893.
Fu, Y.L., Yu, G.R., Sun, X.M., Li, Y.N., Wen, X.F., Zhang, L.M., Li, Z.Q., Zhao, L., Hao, Y.B., 2006a. Depression of net ecosystem CO_2 exchange in semi-arid *Leymus chinensis* steppe and alpine shrub. Agric. For. Meteorol. 137, 234–244.
Fu, Y.L., Yu, G.R., Wang, Y.F., Li, Z.Q., Hao, Y.B., 2006b. Effect of water stress on ecosystem photosynthesis and respiration of a *Leymus chinensis* steppe in Inner Mongolia. Sci. China Ser. D 49, 196–206.
Garbulsky, M.F., Penuelas, J., Papale, D., Ardo, J., Goulden, M.L., Kiely, G., Richardson, A.D., Rotenberg, E., Veenendaal, E.M., Filella, I., 2010. Patterns and controls of the variability of radiation use efficiency and primary productivity across terrestrial ecosystems. Glob. Ecol. Biogeogr. 19, 253–267.
Gockede, M., Foken, T., Aubinet, M., Aurela, M., Banza, J., Bernhofer, C., Bonnefond, J.M., Brunet, Y., Carrara, A., Clement, R., Dellwik, E., Elbers, J., Eugster, W., Fuhrer, J., Granier, A., Grunwald, T., Heinesch, B., Janssens, I.A., Knohl, A., Koeble, R., Laurila, T., Longdoz, B., Manca, G., Marek, M., Markkanen, T., Mateus, J., Matteucci, G., Mauder, M., Migliavacca, M., Minerbi, S., Moncrieff, J., Montagnani, L., Moors, E., Ourcival, J.M., Papale, D., Pereira, J., Pilegaard, K., Pita, G., Rambal, S., Rebmann, C., Rodrigues, A., Rotenberg, E., Sanz, M.J., Sedlak, P., Seufert, G., Siebicke, L., Soussana, J.F., Valentini, R., Vesala, T., Verbeeck, H., Yakir, D., 2008. Quality control of CarboEurope flux data – part 1: coupling footprint analyses with flux data quality assessment to evaluate sites in forest ecosystems. Biogeosciences 5, 433–450.
Greenwald, R., Bergin, M.H., Xu, J., Cohan, D., Hoogenboom, G., Chameides, W.L., 2006. The influence of aerosols on crop production: a study using the CERES crop model. Agric. Syst. 89, 390–413.
Gu, L.H., Baldocchi, D., Verma, S.B., Black, T.A., Vesala, T., Falge, E.M., Dowty, P.R., 2002. Advantages of diffuse radiation for terrestrial ecosystem productivity. J. Geophys. Res.: Atmos. 107 .
Gu, L.H., Baldocchi, D.D., Wofsy, S.C., Munger, J.W., Michalsky, J.J., Urbanski, S.P., Boden, T.A., 2003. Response of a deciduous forest to the Mount Pinatubo eruption: enhanced photosynthesis. Science 299, 2035–2038.
Guan, D.X., Wu, J.B., Zhao, X.S., Han, S.J., Yu, G.R., Sun, X.M., Jin, C.J., 2006. CO_2 fluxes over an old, temperate mixed forest in northeastern China. Agric. For. Meteorol. 137, 138–149.
Hao, Y.B., Wang, Y.F., Huang, X.Z., Cui, X.Y., Zhou, X.Q., Wang, S.P., Niu, H.S., Jiang, G.M., 2007. Seasonal and interannual variation in water vapor and energy exchange over a typical steppe in Inner Mongolia, China. Agric. For. Meteorol. 146, 57–69.
He, M.Z., Ju, W.M., Zhou, Y.L., Chen, J.M., He, H.L., Wang, S.Q., Wang, H.M., Guan, D.X., Yan, J.H., Li, Y.N., Hao, Y.B., Zhao, F.H., 2013. Development of a two-leaf light use efficiency model for improving the calculation of terrestrial gross primary productivity. Agric. For. Meteorol. 173, 28–39.
Heald, C.L., Henze, D.K., Horowitz, L.W., Feddema, J., Lamarque, J.F., Guenther, A., Hess, P.G., Vitt, F., Seinfeld, J.H., Goldstein, A.H., Fung, I., 2008. Predicted change in global secondary organic aerosol concentrations in response to future climate, emissions, and land use change. J. Geophys. Res.: Atmos. 113 .
Heinsch, F.A., Reeves, M., Votava, P., Kang, S., Milesi, C., Zhao, M., Glassy, J., Jolly, W.M., Loehman, R., Bowker, C.F., 2003. GPP and NPP (MOD17A2/A3) Products NASA MODIS Land Algorithm. MOD17 User's Guide, pp. 1–57.
Huang, K., Wang, S.Q., Zhou, L., Wang, H.M., Zhang, J.H., Yan, J.H., Zhao, L., Wang, Y.F., Shi, P.L., 2014. Impacts of diffuse radiation on light use efficiency across terrestrial ecosystems based on eddy covariance observation in China. PLOS ONE 9 .
Kanniah, K., Beringer, J., Tapper, N., Long, C., 2010. Aerosols and their influence on radiation partitioning and savanna productivity in northern Australia. Theor. Appl. Climatol. 100, 423–438.
Kanniah, K.D., Beringer, J., Hutley, L., 2013. Exploring the link between clouds, radiation, and canopy productivity of tropical savannas. Agric. For. Meteorol. 182–183, 304–313.
Kanniah, K.D., Beringer, J., Hutley, L.B., Tapper, N.J., Zhu, X., 2009. Evaluation of Collections 4 and 5 of the MODIS Gross Primary Productivity product and algorithm improvement at a tropical savanna site in northern Australia. Remote Sens. Environ. 113, 1808–1822.
Kanniah, K.D., Beringer, J., North, P., Hutley, L., 2012. Control of atmospheric particles on diffuse radiation and terrestrial plant productivity: a review. Prog. Phys. Geogr. 36, 209–237.
Kim, S.W., Jefferson, A., Yoon, S.C., Dutton, E.G., Ogren, J.A., Valero, F.P.J., Kim, J., Holben, B.N., 2005. Comparisons of aerosol optical depth and surface shortwave irradiance and their effect on the aerosol surface radiative forcing estimation. J. Geophys. Res.: Atmos. 110 .
Kimball, J.S., Thornton, P.E., White, M.A., Running, S.W., 1997. Simulating forest productivity and surface–atmosphere carbon exchange in the BOREAS study region. Tree Physiol. 17, 589–599.
King, D.A., Turner, D.P., Ritts, W.D., 2011. Parameterization of a diagnostic carbon cycle model for continental scale application. Remote Sens. Environ. 115, 1653–1664.
Krinner, G., Viovy, N., de Noblet-Ducoudre, N., Ogee, J., Polcher, J., Friedlingstein, P., Ciais, P., Sitch, S., Prentice, I.C., 2005. A dynamic global vegetation model for studies of the coupled atmosphere-biosphere system. Glob. Biogeochem. Cycles 19 .
Landsberg, J.J., Waring, R.H., 1997. A generalised model of forest productivity using simplified concepts of radiation-use efficiency, carbon balance and partitioning. For. Ecol. Manage. 95, 209–228.
Leuning, R., Cleugh, H.A., Zegelin, S.J., Hughes, D., 2005. Carbon and water fluxes over a temperate Eucalyptus forest and a tropical wet/dry savanna in Australia: measurements and comparison with MODIS remote sensing estimates. Agric. For. Meteorol. 129, 151–173.
Li, H., Qiu, J.J., Wang, L.G., Tang, H.J., Li, C.S., Van Ranst, E., 2010. Modelling impacts of alternative farming management practices on greenhouse gas emissions from a winter wheat-maize rotation system in China. Agric. Ecosyst. Environ. 135, 24–33.
Li, J., Yu, Q., Sun, X.M., Tong, X.J., Ren, C.Y., Wang, J., Liu, E.M., Zhu, Z.L., Yu, G.R., 2006. Carbon dioxide exchange and the mechanism of environmental control in a farmland ecosystem in North China Plain. Sci. China Ser. D 49, 226–240.
Li, Z.Q., Yu, G.R., Xiao, X.M., Li, Y.N., Zhao, X.Q., Ren, C.Y., Zhang, L.M., Fu, Y.L., 2007. Modeling gross primary production of alpine ecosystems in the Tibetan Plateau using MODIS images and climate data. Remote Sens. Environ. 107, 510–519.
Liu, J.F., Chen, S.P., Han, X.G., 2012. Modeling gross primary production of two steppes in Northern China using MODIS time series and climate data. Procedia Environ. Sci. 13, 742–754.
Liu, S.G., Bliss, N., Sundquist, E., Huntington, T.G., 2003. Modeling carbon dynamics in vegetation and soil under the impact of soil erosion and deposition. Glob. Biogeochem. Cycles 17 .
Lloyd, J., Taylor, J.A., 1994. On the temperature dependence of soil respiration. Funct. Ecol. 8, 315–323.
Matsui, K., Umemura, Y., Ohme-Takagi, M., 2008. AtMYBL2, a protein with a single MYB domain, acts as a negative regulator of anthocyanin biosynthesis in Arabidopsis. Plant J. 55, 954–967.
Mercado, L.M., Bellouin, N., Sitch, S., Boucher, O., Huntingford, C., Wild, M., Cox, P.M., 2009. Impact of changes in diffuse radiation on the global land carbon sink. Nature 458, 1014–1087.
Misson, L., Lunden, M., McKay, M., Goldstein, A.H., 2005. Atmospheric aerosol light scattering and surface wetness influence the diurnal pattern of net ecosystem exchange in a semi-arid ponderosa pine plantation. Agric. For. Meteorol. 129, 69–83.
Monteith, J.L., 1972. Solar radiation and productivity in tropical ecosystems. J. Appl. Ecol. 9, 747–766.
Monteith, J.L., Moss, C.J., 1977. Climate and the efficiency of crop production in britain [and discussion]. Philos. Trans. R. Soc. Lond. B Biol. Sci. 281, 277–294.
Mullen, K., Ardia, D., Gil, D., Windover, D., Cline, J., 2011. DEoptim: an R package for global optimization by differential evolution. J. Stat. Softw. 40, 1–26.
Nemani, R.R., Keeling, C.D., Hashimoto, H., Jolly, W.M., Piper, S.C., Tucker, C.J., Myneni, R.B., Running, S.W., 2003. Climate-driven increases in global terrestrial net primary production from 1982 to 1999. Science 300, 1560–1563.
Ogutu, B.O., Dash, J., 2013. Assessing the capacity of three production efficiency models in simulating gross carbon uptake across multiple biomes in conterminous USA. Agric. For. Meteorol. 174, 158–169.
Oliphant, A.J., Dragoni, D., Deng, B., Grimmond, C.S.B., Schmid, H.P., Scott, S.L., 2011. The role of sky conditions on gross primary production in a mixed deciduous forest. Agric. For. Meteorol. 151, 781–791.
Osmond, B., Ananyev, G., Berry, J., Langdon, C., Kolber, Z., Lin, G.H., Monson, R., Nichol, C., Rascher, U., Schurr, U., Smith, S., Yakir, D., 2004. Changing the way we think about global change research: scaling up in experimental ecosystem science. Glob. Change Biol. 10, 393–407.
Piao, S.L., Fang, J.Y., Ciais, P., Peylin, P., Huang, Y., Sitch, S., Wang, T., 2009. The carbon balance of terrestrial ecosystems in China. Nature 458, 1009–1082.
Price, K., Storn, R., Lampinen, J., 2005. Differential Evolution: A Practical Approach to Global Optimization. Springer-Verlag.
Prince, S.D., Goward, S.N., 1995. Global primary production: a remote sensing approach. J. Biogeogr. 22, 815–835.
Raupach, M.R., Canadell, J.G., Le Quere, C., 2008. Anthropogenic and biophysical contributions to increasing atmospheric CO_2 growth rate and airborne fraction. Biogeosciences 5, 1601–1613.
Reichstein, M., Falge, E., Baldocchi, D., Papale, D., Aubinet, M., Berbigier, P., Bernhofer, C., Buchmann, N., Gilmanov, T., Granier, A., Grunwald, T., Havrankova, K., Ilvesniemi, H., Janous, D., Knohl, A., Laurila, T., Lohila, A., Loustau, D., Matteucci, G., Meyers, T., Miglietta, F., Ourcival, J.M., Pumpanen, J., Rambal, S., Rotenberg, E., Sanz, M., Tenhunen, J., Seufert, G., Vaccari, F., Vesala, T., Yakir, D., Valentini, R., 2005. On the separation of net ecosystem exchange into assimilation and ecosystem respiration: review and improved algorithm. Glob. Change Biol. 11, 1424–1439.
Ren, X.L., He, H.L., Zhang, L., Zhou, L., Yu, G.R., Fan, J.W., 2013. Spatiotemporal variability analysis of diffuse radiation in China during 1981–2010. Ann. Geophys. 31, 277–289.
Roderick, M.L., Farquhar, G.D., Berry, S.L., Noble, I.R., 2001. On the direct effect of clouds and atmospheric particles on the productivity and structure of vegetation. Oecologia 129, 21–30.
Rossini, M., Cogliati, S., Meroni, M., Migliavacca, M., Galvagno, M., Busetto, L., Cremonese, E., Julitta, T., Siniscalco, C., Morra di Cella, U., Colombo, R., 2012. Remote sensing-based estimation of gross primary production in a subalpine grassland. Biogeosciences 9, 2565–2584.

Ruimy, A., Dedieu, G., Saugier, B., 1996. TURC: a diagnostic model of continental gross primary productivity and net primary productivity. Glob. Biogeochem. Cycles 10, 269–285.
Running, S.W., Nemani, R.R., Heinsch, F.A., Zhao, M.S., Reeves, M., Hashimoto, H., 2004. A continuous satellite-derived measure of global terrestrial primary production. Bioscience 54, 547–560.
Running, S.W., Thornton, P.E., Nemani, R., Glassy, J.M., 2000. Global terrestrial gross and net primary productivity from the Earth Observing SystemIn: Methods in Ecosystem Science, pp. 44–57.
Sakowska, K., Vescovo, L., Marcolla, B., Juszczak, R., Olejnik, J., Gianelle, D., 2014. Monitoring of carbon dioxide fluxes in a subalpine grassland ecosystem of the Italian Alps using a multispectral sensor. Biogeosciences 11, 4695–4712.
Schaefer, K., Schwalm, C.R., Williams, C., Arain, M.A., Barr, A., Chen, J.M., Davis, K.J., Dimitrov, D., Hilton, T.W., Hollinger, D.Y., Humphreys, E., Poulter, B., Raczka, B.M., Richardson, A.D., Sahoo, A., Thornton, P., Vargas, R., Verbeeck, H., Anderson, R., Baker, I., Black, T.A., Bolstad, P., Chen, J.Q., Curtis, P.S., Desai, A.R., Dietze, M., Dragoni, D., Gough, C., Grant, R.F., Gu, L.H., Jain, A., Kucharik, C., Law, B., Liu, S.G., Lokipitiya, E., Margolis, H.A., Matamala, R., McCaughey, J.H., Monson, R., Munger, J.W., Oechel, W., Peng, C.H., Price, D.T., Ricciuto, D., Riley, W.J., Roulet, N., Tian, H.Q., Tonitto, C., Torn, M., Weng, E.S., Zhou, X.L., 2012. A model-data comparison of gross primary productivity: results from the North American Carbon Program site synthesis. J. Geophys. Res.: Biogeosci. 117 .
Schiermeier, Q., 2006. Oceans cool off in hottest years. Nature 442, 854–855.
Shi, P.L., Sun, X.M., Xu, L.L., Zhang, X.Z., He, Y.T., Zhang, D.Q., Yu, G.R., 2006. Net ecosystem CO_2 exchange and controlling factors in a steppe – Kobresia meadow on the Tibetan Plateau. Sci. China Ser. D 49, 207–218.
Still, C.J., Riley, W.J., Biraud, S.C., Noone, D.C., Buenning, N.H., Randerson, J.T., Torn, M.S., Welker, J., White, J.W.C., Vachon, R., Farquhar, G.D., Berry, J.A., 2009. Influence of clouds and diffuse radiation on ecosystem-atmosphere CO_2 and $CO^{18}O$ exchanges. J. Geophys. Res.: Biogeosci. 114, G01018.
Turner, D.P., Ritts, W.D., Cohen, W.B., Gower, S.T., Running, S.W., Zhao, M.S., Costa, M.H., Kirschbaum, A.A., Ham, J.M., Saleska, S.R., Ahl, D.E., 2006a. Evaluation of MODIS NPP and GPP products across multiple biomes. Remote Sens. Environ. 102, 282–292.
Turner, D.P., Ritts, W.D., Styles, J.M., Yang, Z., Cohen, W.B., Law, B.E., Thornton, P.E., 2006b. A diagnostic carbon flux model to monitor the effects of disturbance and interannual variation in climate on regional NEP. Tellus B 58, 476–490.
Turner, D.P., Urbanski, S., Bremer, D., Wofsy, S.C., Meyers, T., Gower, S.T., Gregory, M., 2003. A cross-biome comparison of daily light use efficiency for gross primary production. Glob. Change Biol. 9, 383–395.
Urban, O., Janous, D., Acosta, M., Czerny, R., Markova, I., Navratil, M., Pavelka, M., Pokorny, R., Sprtova, M., Zhang, R., Spunda, V., Grace, J., Marek, M.V., 2007. Ecophysiological controls over the net ecosystem exchange of mountain spruce stand. Comparison of the response in direct vs. diffuse solar radiation. Glob. Change Biol. 13, 157–168.
Urban, O., Klem, K., Holišová, P., Šigut, L., Šprtová, M., Teslová-Navrátilová, P., Zitová, M., Špunda, V., Marek, M.V., Grace, J., 2014. Impact of elevated CO_2 concentration on dynamics of leaf photosynthesis in *Fagus sylvatica* is modulated by sky conditions. Environ. Pollut. 185, 271–280.
Veroustraete, F., Sabbe, H., Eerens, H., 2002. Estimation of carbon mass fluxes over Europe using the C-Fix model and Euroflux data. Remote Sens. Environ. 83, 376–399.
Webb, E.K., Pearman, G.I., Leuning, R., 1980. Correction of flux measurements for density effects due to heat and water vapour transfer. Q. J. R. Meteorol. Soc. 106, 85–100.
Wen, X.F., Wang, H.M., Wang, J.L., Yu, G.R., Sun, X.M., 2010. Ecosystem carbon exchanges of a subtropical evergreen coniferous plantation subjected to seasonal drought, 2003–2007. Biogeosciences 7, 357–369.
Wu, C.Y., Munger, J.W., Niu, Z., Kuang, D., 2010a. Comparison of multiple models for estimating gross primary production using MODIS and eddy covariance data in Harvard Forest. Remote Sens. Environ. 114, 2925–2939.
Wu, C.Y., Niu, Z., Gao, S.A., 2010b. Gross primary production estimation from MODIS data with vegetation index and photosynthetically active radiation in maize. J. Geophys. Res.: Atmos. 115 .
Wu, J.B., Xiao, X.M., Guan, D.X., Shi, T.T., Jin, C.J., Han, S.J., 2008a. Estimation of the gross primary production of an old-growth temperate mixed forest using eddy covariance and remote sensing. Int. J. Remote Sens. 30, 463–479.
Wu, W.X., Wang, S.Q., Xiao, X.M., Yu, G.R., Fu, Y.L., Hao, Y.B., 2008b. Modeling gross primary production of a temperate grassland ecosystem in Inner Mongolia, China, using MODIS imagery and climate data. Sci. China Ser. D 51, 1501–1512.
Xiao, J.F., Davis, K.J., Urban, N.M., Keller, K., Saliendra, N.Z., 2011. Upscaling carbon fluxes from towers to the regional scale: influence of parameter variability and land cover representation on regional flux estimates. J. Geophys. Res.: Biogeosci. 116 .
Xiao, J.F., Zhuang, Q.L., Baldocchi, D.D., Law, B.E., Richardson, A.D., Chen, J.Q., Oren, R., Starr, G., Noormets, A., Ma, S.Y., Verma, S.B., Wharton, S., Wofsy, S.C., Bolstad, P.V., Burns, S.P., Cook, D.R., Curtis, P.S., Drake, B.G., Falk, M., Fischer, M.L., Foster, D.R., Gu, L.H., Hadley, J.L., Hollinger, D.Y., Katul, G.G., Litvak, M., Martin, T.A., Matamala, R., McNulty, S., Meyers, T.P., Monson, R.K., Munger, J.W., Oechel, W.C., Paw U, K.T., Schmid, H.P., Scott, R.L., Sun, G., Suyker, A.E., Torn, M.S., 2008. Estimation of net ecosystem carbon exchange for the conterminous United States by combining MODIS and AmeriFlux data. Agric. For. Meteorol. 148, 1827–1847.
Xiao, X.M., Hollinger, D., Aber, J., Goltz, M., Davidson, E.A., Zhang, Q.Y., Moore, B., 2004. Satellite-based modeling of gross primary production in an evergreen needleleaf forest. Remote Sens. Environ. 89, 519–534.
Yan, H., Wang, S.Q., Billesbach, D., Oechel, W., Bohrer, G., Meyers, T., Martin, T.A., Matamala, R., Phillips, R.P., Rahman, F., Yu, Q., Shugart, H.H., 2015. Improved global simulations of gross primary product based on a new definition of water stress factor and a separate treatment of C3 and C4 plants. Ecol. Model. 297, 42–59.
Yan, H., Wang, S.Q., Billesbach, D., Oechel, W., Zhang, J.H., Meyers, T., Martin, T.A., Matamala, R., Baldocchi, D., Bohrer, G., Dragoni, D., Scott, R., 2012. Global estimation of evapotranspiration using a leaf area index-based surface energy and water balance model. Remote Sens. Environ. 124, 581–595.
Yan, H.M., Fu, Y.L., Xiao, X.M., Huang, H.Q., He, H.L., Ediger, L., 2009. Modeling gross primary productivity for winter wheat-maize double cropping system using MODIS time series and CO_2 eddy flux tower data. Agric. Ecosyst. Environ. 129, 391–400.
Yang, X.J., Wittig, V., Jain, A.K., Post, W., 2009. Integration of nitrogen cycle dynamics into the Integrated Science Assessment Model for the study of terrestrial ecosystem responses to global change. Glob. Biogeochem. Cycles 23 .
Yang, Y.T., Shang, S.H., Guan, H.D., Jiang, L., 2013. A novel algorithm to assess gross primary production for terrestrial ecosystems from MODIS imagery. J. Geophys. Res.: Biogeosci. 118, 590–605.
Yu, G.R., Song, X., Wang, Q.F., Liu, Y.F., Guan, D.X., Yan, J.H., Sun, X.M., Zhang, L.M., Wen, X.F., 2008a. Water-use efficiency of forest ecosystems in eastern China and its relations to climatic variables. New Phytol. 177, 927–937.
Yu, G.R., Wen, X.F., Sun, X.M., Tanner, B.D., Lee, X.H., Chen, J.Y., 2006. Overview of ChinaFLUX and evaluation of its eddy covariance measurement. Agric. For. Meteorol. 137, 125–137.
Yu, G.R., Zhang, L.M., Sun, X.M., Fu, Y.L., Wen, X.F., Wang, Q.F., Li, S.G., Ren, C.Y., Song, X., Liu, Y.F., Han, S.J., Yan, J.H., 2008b. Environmental controls over carbon exchange of three forest ecosystems in eastern China. Glob. Change Biol. 14, 2555–2571.
Yu, G.R., Zhu, X.J., Fu, Y.L., He, H.L., Wang, Q.F., Wen, X.F., Li, X.R., Zhang, L.M., Zhang, L., Su, W., Li, S.G., Sun, X.M., Zhang, Y.P., Zhang, J.H., Yan, J.H., Wang, H.M., Zhou, G.S., Jia, B.R., Xiang, W.H., Li, Y.N., Zhao, L., Wang, Y.F., Shi, P.L., Chen, S.P., Xin, X.P., Zhao, F.H., Wang, Y.Y., Tong, C.L., 2013. Spatial patterns and climate drivers of carbon fluxes in terrestrial ecosystems of China. Glob. Change Biol. 19, 798–810.
Yuan, W.P., Cai, W.W., Xia, J.Z., Chen, J.Q., Liu, S.G., Dong, W.J., Merbold, L., Law, B., Arain, A., Beringer, J., Bernhofer, C., Black, A., Blanken, P.D., Cescatti, A., Chen, Y., Francois, L., Gianelle, D., Janssens, I.A., Jung, M., Kato, T., Kiely, G., Liu, D., Marcolla, B., Montagnani, L., Raschi, A., Roupsard, O., Varlagin, A., Wohlfahrt, G., 2014. Global comparison of light use efficiency models for simulating terrestrial vegetation gross primary production based on the La Thuile database. Agric. For. Meteorol. 192, 108–120.
Yuan, W.P., Liu, S., Zhou, G.S., Zhou, G.Y., Tieszen, L.L., Baldocchi, D., Bernhofer, C., Gholz, H., Goldstein, A.H., Goulden, M.L., Hollinger, D.Y., Hu, Y., Law, B.E., Stoy, P.C., Vesala, T., Wofsy, S.C., 2007. Deriving a light use efficiency model from eddy covariance flux data for predicting daily gross primary production across biomes. Agric. For. Meteorol. 143, 189–207.
Zhang, L.-M., Yu, G.-R., Sun, X.-M., Wen, X.-F., Ren, C.-Y., Fu, Y.-L., Li, Q.-K., Li, Z.-Q., Liu, Y.-F., Guan, D.-X., Yan, J.-H., 2006a. Seasonal variations of ecosystem apparent quantum yield (α) and maximum photosynthesis rate (Pmax) of different forest ecosystems in China. Agric. For. Meteorol. 137, 176–187.
Zhang, L.M., Yu, G.R., Sun, X.M., Wen, X.F., Ren, C.Y., Song, X., Liu, Y.F., Guan, D.X., Yan, J.H., Zhang, Y.P., 2006b. Seasonal variation of carbon exchange of typical forest ecosystems along the eastern forest transect in China. Sci. China Ser. D 49, 47–62.
Zhang, M., Yu, G.-R., Zhuang, J., Gentry, R., Fu, Y.-L., Sun, X.-M., Zhang, L.-M., Wen, X.-F., Wang, Q.-F., Han, S.-J., Yan, J.-H., Zhang, Y.-P., Wang, Y.-F., Li, Y.-N., 2011. Effects of cloudiness change on net ecosystem exchange, light use efficiency, and water use efficiency in typical ecosystems of China. Agric. For. Meteorol. 151, 803–816.
Zhang, Y.Q., Yu, Q., Jiang, J., Tang, Y.H., 2008. Calibration of Terra/MODIS gross primary production over an irrigated cropland on the North China Plain and an alpine meadow on the Tibetan Plateau. Glob. Change Biol. 14, 757–767.
Zhao, M.S., Heinsch, F.A., Nemani, R.R., Running, S.W., 2005. Improvements of the MODIS terrestrial gross and net primary production global data set. Remote Sens. Environ. 95, 164–176.